Japanese Journal of Applied Physics

The Japan Society of Applied Physics

Band-Gap Energy Anomaly and Sublattice Ordering in GaInP and AlGaInP Grown by Metalorganic Vapor Phase Epitaxy

To cite this article: Tohru Suzuki *et al* 1988 *Jpn. J. Appl. Phys.* **27** 2098

View the article online for updates and enhancements.

You may also like

- Recovering the efficiency of AlGaInP red micro-LEDs using sidewall treatments
Matthew S. Wong, Ryan C. White, Stephen Gee et al.
- Recent progress in red light-emitting diodes by III-nitride materials
Daisuke Iida and Kazuhiro Ohkawa
- Effect of n-Type AlGaAs Layer on Efficiency of Reflective 590-nm AlGaInP Light Emitting Diodes
Hyung Joo Lee, Jae Hoon Kim and Choong Hun Lee

This content was downloaded from IP address 18.117.76.7 on 30/04/2024 at 22:05

JAPANESE JOURNAL OF APPLIED PHYSICS
VOL. 27, NO. 11, NOVEMBER, 1988, pp. 2098-2106

Band-Gap Energy Anomaly and Sublattice Ordering in GaInP and AlGaInP Grown by Metalorganic Vapor Phase Epitaxy

Tohru SUZUKI, Akiko GOMYO, Sumio IIJIMA,†
Kenichi KOBAYASHI, Seiji KAWATA, Isao HINO††
and Tonao YUASA

Opto-electronics Research Laboratories, NEC Corporation,
†Fundamental Research Laboratories, NEC Corporation,
††Compound Semiconductor Device Division, NEC Corporation,
1-1, Miyazaki 4-chome, Miyamae-ku, Kawasaki 213

(Received May 18, 1988; accepted for publication September 17, 1988)

The previously reported photoluminescence(PL)-peak-energy anomaly problem for $Ga_{0.5}In_{0.5}P$ grown on GaAs by metalorganic vapor phase epitaxy (MOVPE) was studied in detail. X-ray microprobe analysis, and optical transmisson spectra measurements were carried out to examine alloy compositions and band-gap energies (E_gs), respectively. The MOVPE growth condition dependence of $\{1/2, 1/2, 1/2\}$ superlattices (SLs) on the cation sublattice in $Ga_{0.5}In_{0.5}P$ was studied in detail, using transmission electron microscopy. The correlation between the E_g anomaly and the SLs was examined in detail and established. Raman spectra seemed to show zone-folding effects due to the monolayer SL. A similar E_g anomaly was reported for AlGaInP. AlGaInP and AlInP were also found to show the same SLs.

KEYWORDS: GaInP, AlGaInP, AlInP, sublattice ordering, monolayer superlattice, MOVPE, band-gap energy, Raman scattering spectrum, TEM, XMA

§1. Introduction

In spite of the firm belief, which had generally been held by most workers in this field, that a ternary III-V compound with a certain alloy composition should have a corresponding unique band-gap energy value, it has been reported that $Ga_{0.5}In_{0.5}P$ grown on (001) GaAs by metalorganic vapor phase epitaxy (MOVPE) can have an arbitrary band-gap energy value from about 1.85 to 1.9 eV, depending on the MOVPE growth conditions, such as growth temperature[1,2,3),*,**] and V/III ratio.[1,2)] A generally accepted band-gap energy is 1.9~1.92 eV.[4,5,6)] This band-gap energy anomaly has been called the "50 meV problem".[1)]

In a previous report,[1)] it was pointed out that a composition, which is determined from X-ray diffraction measurement, will still allow some freedom in determining extremely small-scale (on the order of lattice spacing) configurations for Ga and In on a group III element sublattice. It was also asserted that this atomic-scale configuration difference can be the cause of the band-gap energy difference. An anomalously low E_g was found to change into a normal E_g by diffusing Zn into the $Ga_{0.5}In_{0.5}P$.[2)] This observation was strong support for the assertion, suggesting that some atomic scale structure on the column III sublattice accompanied by an abnormal E_g is converted by the Zn diffusion to a random configuration for Ga and In on the sublattice.

It was concluded that epitaxial layers with anomalous and normal band-gaps may have an ordered and a random(Ga, In) distribution on the column III sublattice, respectively.[2)] Moreover, the band-gap energy anomaly was suggested to have a correlation with the bilayer superlattice GaGaInInGaGaInIn . . . on the $(\bar{1}10)$ plane.[2)] This suggestion, however, was made based only on [001] and $[\bar{1}10]$ zone axes TEM (transmission electron microscope) observations for $Ga_{0.5}In_{0.5}P$ grown at temperatures higher than 650°C. This assertion was found not to be the case for growth temperatures $\lesssim$600°C.[7,8)] After the report, in the [110] zone axis, we first observed extremely strong superstructure spots: $h\mp1/2$, $k\pm1/2$, $1+1/2$ for $Ga_{0.5}In_{0.5}P$ with an anomalously low band-gap energy ~1.85 eV, where h, k, and l are all even or all odd integers.[9),*] This observation indicates that naturally formed $(\mp1/2, \pm1/2, 1/2)$** superlattices (SLs) of the sequence (Ga plane)(In plane)(Ga plane)(In plane) . . . in the $[\bar{1}11]$ or $[1\bar{1}1]$ directions are responsible for the band-gap energy (E_g) anomaly.

The purpose of this paper is to coherently describe the E_g anomaly and the sublattice ordering observed in $Ga_{0.5}In_{0.5}P$, i.e. to supplement and reinforce the description of the "50 meV problem" with new data and to give a detailed description of the relation between the E_g and the atom ordering on the column III sublattice. The relation between the formerly observed SL and the newly observed {111} SL is discussed. A similar E_g anomaly problem and sublattice orderings in $(Al_xGa_{1-x})_{0.5}In_{0.5}P$ lattice-matched to GaAs substrate, are also described.

In §2, experimental methods are described. In §3, ex-

*In Fig. 2 in Ref. 2 (Appl. Phys. Lett.), the [110] and $[\bar{1}10]$ directions should be reversed in order to be consistent with the present notation.

**Strictly, in Ref. 3, there is no description claiming that the anomalous photoluminescence peak energy corresponds to an anomaly in band-gap energy.

*The TED pattern of the $\{1/2, 1/2, 1/2\}$ superlattice and its correlation with E_g anomaly were first reported by T. Suzuki, A. Gomyo, K. Kobayashi, S. Kawata, I. Hino, and T. Yuasa in an invited talk (in Japanese) at the 7th Meeting of Monbusyo Special Project Research on Alloy Semiconductor Physics and Electronics, Kohfu, Yamanashi, Japan, July, 1987.

**Hereafter, $(\bar{1}/2, 1/2, 1/2)$ is represented as $(\bar{1}11)$, for simplicity.

perimental results together with some detailed and critical descriptions are given for the band-gap energy anomaly and crystal structure analysis by TEM observation. The relation between the band-gap energy anomaly and the sublattice ordering is discussed. Summary and conclusion are given in §4.

§2. Experiments

Low-pressure (70 Torr) MOVPE was used to grow $Ga_{0.5}In_{0.5}P$, $(Al_xGa_{1-x})_{0.5}In_{0.5}P$ and $Al_{0.5}In_{0.5}P$ layers, using a horizontal quartz reactor. GaAs substrates oriented (001) 2° off towards [011] were used in this study, unless otherwise mentioned.* The growths were carried out at temperatures(T_g) ranging from 550°C to 750°C. The column V to column III element source-gas partial-pressure ratio (V/III ratio) was varied from 60 to 400, by changing the phosphine (PH_3) partial pressure. The growth rate was $\sim 1\,\mu m/h$. The thicknesses of the epitaxial layers were $0.5 \sim 1\,\mu m$. Other growth conditions have been described in a separate paper.[1)]

Ternary alloy composition (x) was determined by measuring the lattice-mismatching degree with a double-crystal X-ray diffractometer, using $CuK_{\alpha 1}$ line and (004) reflection, and by assuming Vegard's law. It was assumed that $(\Delta a/a)_\perp = 2 \cdot (\Delta a/a)_f$, where $(\Delta a/a)_\perp$ is the mismatch of the lattice constant of the epitaxial layer and its substrate at a right angle to the interface between the epitaxial layer and the substrate and $(\Delta a/a)_f$ is the mismatch of the lattice constant of a free layer. X-ray micro-analyses (XMA) were carried out in order to check the validity of the alloy composition determination by lattice constant measurements.

Photoluminescence (PL) measurements were carried out by using an Ar ion laser as an excitation source. The 300 K E_g was determined by measuring PL peak energy. The E_g value for a sample with some lattice mismatching from a GaAs substrate was corrected to the E_g value corresponding to the lattice-matching composition ($x \cong 0.516$), by using Vegard's law and the E_g-vs-composition(x) relation[6)] for $Ga_xIn_{1-x}P$.

Optical transmission spectra were taken by removing GaAs substrates by chemical wet etching. The samples were thinned to a thickness less than $0.1\,\mu m$ by the chemical wet etching, in order to reduce an optical interference effect between front and back surfaces. Raman scattering spectra were measured in the similar way to that reported in the previous work.[1)]

Cross-sectional samples for [110] and [$\bar{1}$10] zone-axis TEM observations were prepared by mechanical polishing and Ar ion etching. Chemical wet etching was used for [001] zone-axis plane-view observations. The Akashi 002B and JEOL 4000EX electron microscopes were employed.

§3. Results and Discussion

3.1 *Band-gap energy (E_g) anomaly*

3.1.1 *$Ga_{0.5}In_{0.5}P$*

Figure 1 shows 300 K PL peak energy vs growth temperatures (T_g) under three different V/III ratios 62, 230, and ~400. PL peak energy takes minimum values from 1.83 to 1.85 eV at around 650°C for respective V/III ratios. As shown for V/III ~400 case, PL peak energy for crystals grown at higher or lower T_g tends to approach the reported normal value (1.9 ~ 1.92 eV). PL peak energy dependence on the V/III ratio is also observed for a fixed T_g, *e.g.* 700°C.

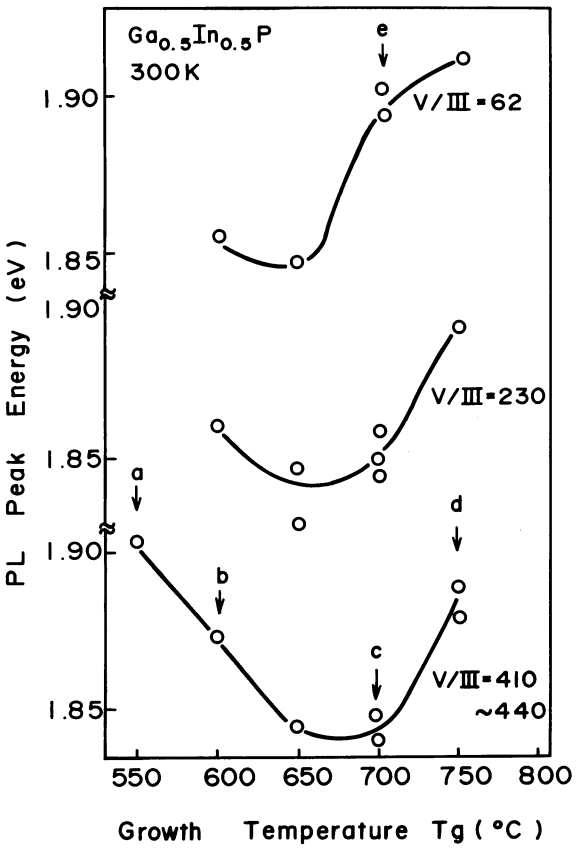

Fig. 1. 300 K PL peak energy for $Ga_{0.5}In_{0.5}P$ as a function of growth temperature (T_g). V/III ratio is taken as a parameter. For arrows with letters, see the caption of Fig. 7.

The alloy compositions shown in Fig. 1 were determined using X-ray diffraction. PL peak energies were corrected in the manner mentioned in §1, as was also done in the previous papers.[1,2)] In order to check the validity of the alloy composition determination by lattice-constant measurements with an X-ray diffractometer, the composition x(XRC) by the diffractometer was compared with the composition x(XMA) determined by XMA, where XRC stands for X-ray rocking curve. Figure 2 shows this comparison. There can be seen an excellent correlation between x(XRC) and x(XMA), as was expected. This fact indicates that x(XRC) can be used for representing the alloy composition. x_0(XRC) means a composition $x \cong 0.516$, for which $Ga_xIn_{1-x}P$ lattice matches the GaAs substrate.[6)]

In Table I, lattice mismatches and 300 K E_g values for $Ga_xIn_{1-x}P$ used for examination (Fig. 2) of the relation between x(XRC) and x(XMA) are summarized. Here, $(dE_g/dx)_{x=0.5} \cong 1.51$ eV is a derivative of $E_g(x)$[6)] with respect to x at $x=0.5$. Using this value, $E_g^{PL}(x)$ is converted to $E_g^{PL}(x_0)$. $E_g^{PL}(x_0)$ is a reduced E_g value, which the

*Substrates used in Ref. 1 were actually (001) 2° off towards [011], in spite of the description therein.

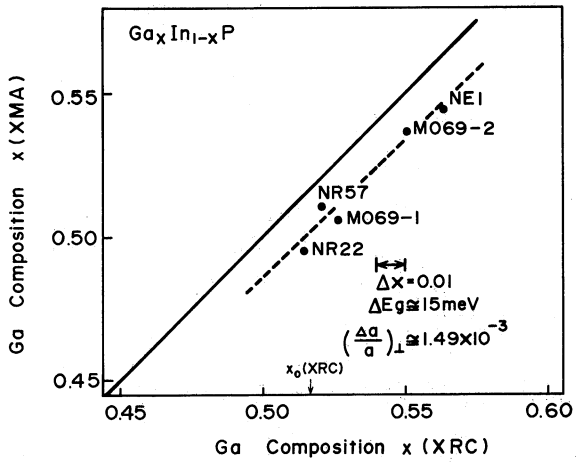

Fig. 2. Ga composition (x) in the $Ga_xIn_{1-x}P$ determined by XMA as a function of that determined by X-ray rocking curve. The x_0 (XRC) meaning is explained in the text. The composition difference of $\Delta x=0.01$ corresponds to ΔE_g 15 mV in band-gap energy, and to $(\Delta a/a)_\perp \cong 1.49\times10^{-3}$ in lattice mismatch.

Table I. Lattice mismatches and E_g(300 K)values for $Ga_xIn_{1-x}P$ used for examination of the relation between x(XRC) and x(XMA).

Sample No.	$(\Delta a/a)_\perp$[a]	x(XRC)[b]	x(XMA)[c]	E_g^{PL}(obs.)[d] (eV)	$E_g^{PL}(x\to x_0)$[e] (eV)
NR22	$+1.7\times10^{-4}$	0.515	0.495	1.900	1.902
NR57	-6.0×10^{-4}	0.521	0.510	1.850	1.842
MO69-1[f]	-1.5×10^{-3}	0.527	0.506	1.862	1.845
MO69-2[g]	-5.2×10^{-3}	0.551	0.535	1.905	1.852
NE1	-7.0×10^{-3}	0.564	0.544	1.906	1.834

[a] Lattice mismatches obtained from (004) X-ray reflection.
[b] Ga compositions in $Ga_xIn_{1-x}P$, determined with $(\Delta a/a)_\perp$ values and Vegard's law.
[c] Ga compositions in $Ga_xIn_{1-x}P$, determined with X-ray microanalysis.
[d] 300 K PL peak energies as observed.
[e] 300 K PL peak energies reduced as follows;

$$E_g^{PL}(x\to x_0)=E_g^{PL}(\text{obs.})-(x-x_0)\left.\frac{dE_g}{dx}\right|_{x=0.5},$$

where x is x(XRC.). Meanings of x_0 and $(dE_g/dx)_{x=0.5}$ are explained in text.
[f,g] Two samples from different places in the same wafer (MO69). MO69 was grown using TEIn and TEGa.

sample would take for the composition x_0. It is observed that samples NR57, MO69-1, MO69-2 and NE1 show anomalous E_g values 1.83 ~ 1.85 eV and that the sample NR22 shows a nearly normal E_g value ~ 1.9 eV. It is thus concluded that a linear relationship between x(XRC) and x(XMA) holds well, regardless of whether E_g values are normal or anomalous.

Another point to be noticed is that two samples, MO69-1 and 2, from the same wafer with different compositions, which resulted from spatial variation in the alloy composition within the same wafer, show approximately the same reduced $E_g^{PL}(x_0)\simeq 1.85$ eV. As the two samples were from the same wafer, the growth conditions were almost the same. The difference in the alloy composition should be the result of the spatial difference in the column III source gas composition on the wafer.

The fact that in spite of the large lattice-mismatch difference among NR57, MO69-1, MO69-2 and NE1, the reduced $E_g^{PL}(x_0)$ values are anomalously low values, means that the anomalous E_g problem occurs regardless of the degree of lattice mismatch, at least up to $|\Delta a/a|_\perp \gtrsim 7\times10^{-3}$. This mismatch is equivalent to 5% in alloy composition.

In a previous paper, PL peak energy values were used as band-gap energy (E_g) values, after some examinations on low-temperature PL spectra, etc.[1] In the present paper, optical transmission spectra are added for samples with and without anomalous PL peak energy. Figure 3 shows 300 K PL spectra (a and b) and corresponding optical transmission (OT) spectra (a′ and b′) for $Ga_{0.5}In_{0.5}P$ layers with an anomalous (1.85 eV) and a normal (1.9 eV) PL peak energy. Growth conditions were T_g 650°C, V/III 230, and T_g 700°C, V/III 60, respectively. The shape of the transmission spectrum a′ is similar to that for b′, but relatively broad compared to b′. The relation between PL spectrum (a) and OT spectrum (a′), however, is very similar to that between those for b and b′; a′ is ~ 50 meV displaced to the lower-energy side as compared to b′. Thus, it is reasonable, as is expected, to assume the PL peak energy as being band-gap energy (E_g). For this reason, hereafter, PL peak energy is called band-gap energy (E_g), as has been done in previous reports.[1,2] The reason for the broadness of the OT spectrum a′ is discussed later in §3.3.

Raman scattering spectra were measured for $Ga_{0.5}In_{0.5}P$ grown under a wide range of growth conditions (T_g from 550 to 750°C and V/III ratio from ~ 60 to ~ 400). Undoped samples were used in order to avoid complex plasmon effects from free carriers, i.e. to see clearly whether this anomalous E_g behavior was related to some atomic structures in the crystals. In Fig. 4, typical Raman scattering spectra for two samples with nearly normal(upper) and anomalous(bottom) E_g values

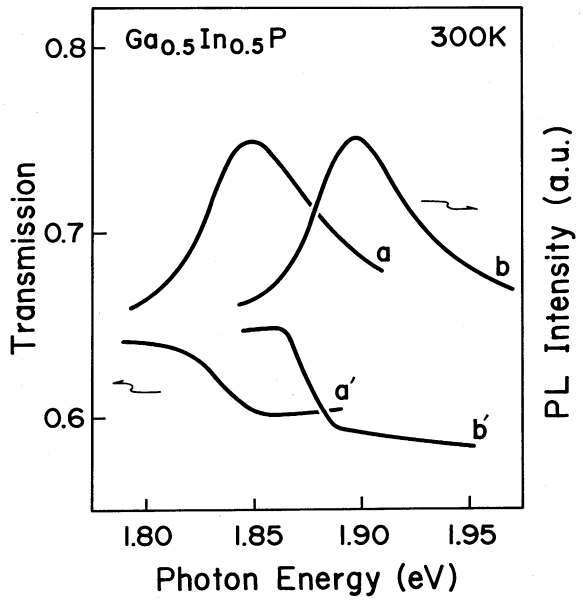

Fig. 3. 300 K PL spectra and corresponding optical transmission spectra for samples with abnormal (a, a′) and normal (b, b′) E_g values. The crystal growth conditions are shown in the text.

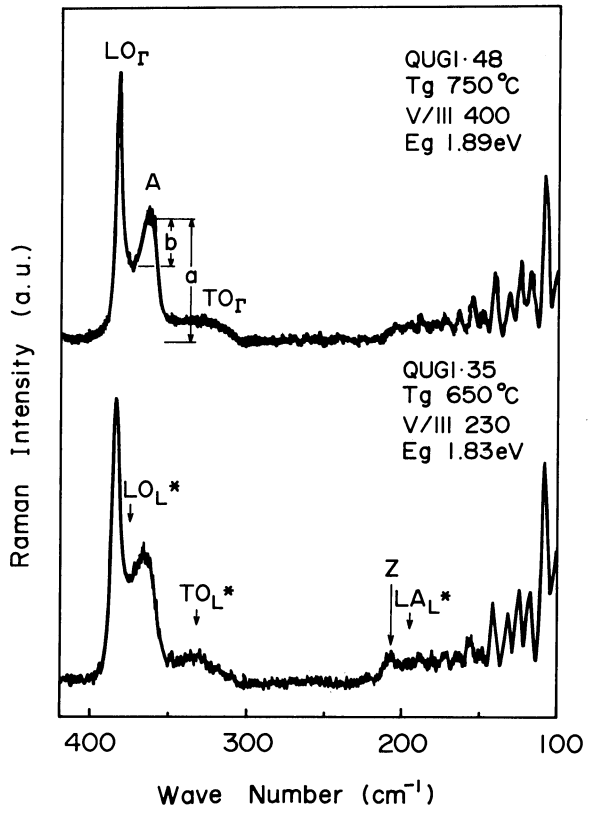

Fig. 4. Raman scattering spectra for samples with normal (upper) and anomalous (bottom) E_g values. Many peaks whose wave numbers are smaller than $\sim 200\ cm^{-1}$ are due to the scattering from air. Symbol meanings are explained in the text (§3.1.1 and §3.3.).

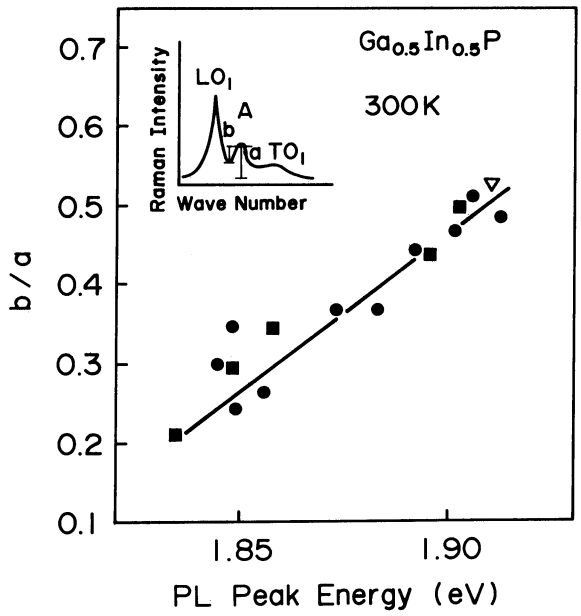

Fig. 5. Relation between "valley depth (b/a)" (defined in the text) and PL peak energy for $Ga_{0.5}In_{0.5}P$ grown under various MOVPE conditions. Open triangle indicates a sample grown by liquid-phase epitaxy. Closed squares indicate samples grown at 700°C and V/III ratio from 62 to ~400. Closed circles indicate samples grown under other various MOVPE conditions: T_g ranging from 550 to 750°C and V/III ratio ranging from 62 to ~400.

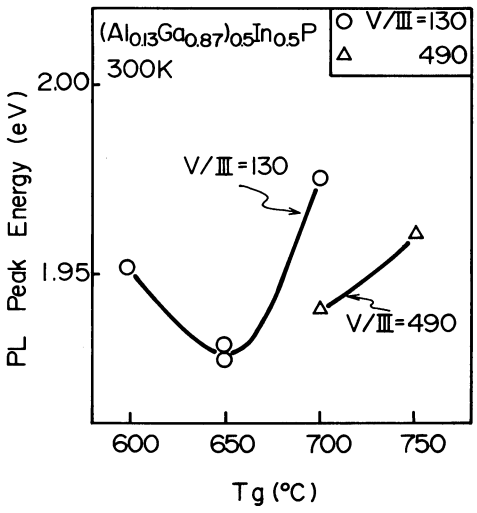

Fig. 6. 300 K PL peak energy for $(Al_{0.13}Ga_{0.87})_{0.5}In_{0.5}P$ as a function of T_g under 130 and 490 V/III ratios.

are shown. First, attention is focused on the quantity of b/a vs E_g, where b/a is the same as that defined in Ref. 1, i.e. the "valley depth" normalized to peak-A intensity.

The results are summarized in Fig. 5. Closed squares indicate the data for samples grown at 700°C under various V/III ratios, from ~60 to ~400, which were previously reported. Closed circles indicate data points for samples grown under various growth conditions: T_g 550~750°C and the V/III ratio from ~60 to ~400. The data for a crystal with a normal E_g value, grown by liquid-phase epitaxy, is also shown (open triangle). An excellent correlation can be observed between E_g (300 K) and the "valley depth"(b/a). Thus, it is quite reasonable to assume that E_g variation for growth condition variation is related to some atomic structure variation.

The second point to be noticed is a spectrum feature around 200 cm^{-1}. In the spectrum for the sample with an anomalous E_g (1.83 eV), there can be seen a small peak at 207 cm^{-1} (indicated as Z in Fig. 4(bottom)). This peak appears consistently for crystals with anomalous E_g values. For the sample with the nearly normal E_g (1.89 eV), however, the peak is virtually not observed (Fig. 4 (upper)). A highly Mg- or Zn-doped ($p \gtrsim 1 \times 10^{18}\ cm^{-3}$) $Ga_{0.5}In_{0.5}P$, grown under a condition in which E_g takes an anomalous value if the crystal is undoped, has been found to show a normal E_g value.[8],* For the highly Zn-doped sample, the peak at 207 cm^{-1} was also observed.

*A. Gomyo, I. Hino, K. Kobayashi, S. Kawata, T. Yuasa and T. Suzuki: Extended Abstracts of the 47th Fall Meeting of Jpn. Soc. Appl. Phys., Sapporo (1986) 27p-Hl (in Japanese).

In this spectrum range, there may be no need to worry about complex free-carrier (hole) plasmon effects due to Zn doping. Thus, the peak Z in Fig. 4(bottom) seems to have a relation to the anomalous E_g problem, as well as the "valley depth (b/a)".

3.1.2 $(Al_xGa_{1-x})_{0.5}In_{0.5}P$

Heretofore, an E_g anomaly has been described for the ternary $Ga_{0.5}In_{0.5}P$. A similar problem occurs in $(Al_xGa_{1-x})_{0.5}In_{0.5}P$. Figure 6 shows E_g dependence on T_g and V/III ratio for $(Al_{0.13}Ga_{0.87})_{0.5}In_{0.5}P$. Although data points are limited compared to the $Ga_{0.5}In_{0.5}P$ case, a similar T_g and V/III dependence is clearly observed.

3.2 *Structure analysis by TEM observation*

3.2.1 $Ga_{0.5}In_{0.5}P$

In Figs. 7(a)~7(e), typical [110] zone axis TED patterns for four $Ga_{0.5}In_{0.5}P$ layers, grown at different T_g values and V/III ratios are shown. The growth conditions for these samples correspond to those indicated by arrows with corresponding letters in Fig. 1. In [$\bar{1}$10] zone-axis TED patterns for these samples, virtually no superstructure was observed. Extremely strong superstructure spots $h-1/2$, $k+1/2$, $1+1/2$ can be seen for 700°C (c), where h, k, and l are all even or all odd integers. Weaker intensity spots $h+1/2$, $k-1/2$, $l+1/2$ are also observed. Hereafter, h,k, and l are omitted for simplicity. These observations indicate that a monolayer SL with a sequence of (Ga plane)(In plane)(Ga plane)(In plane) . . . in the [$\bar{1}$11] direction is dominant on the column III sublattice. In the bottom right of Fig. 7, a structure model for this ($\bar{1}$11) SL, which is projected to the (110) plane, is shown. Weak reflections 0, 0, 1 and 1, 1, 0 in Fig. 7(c) were ascribed to double reflections.

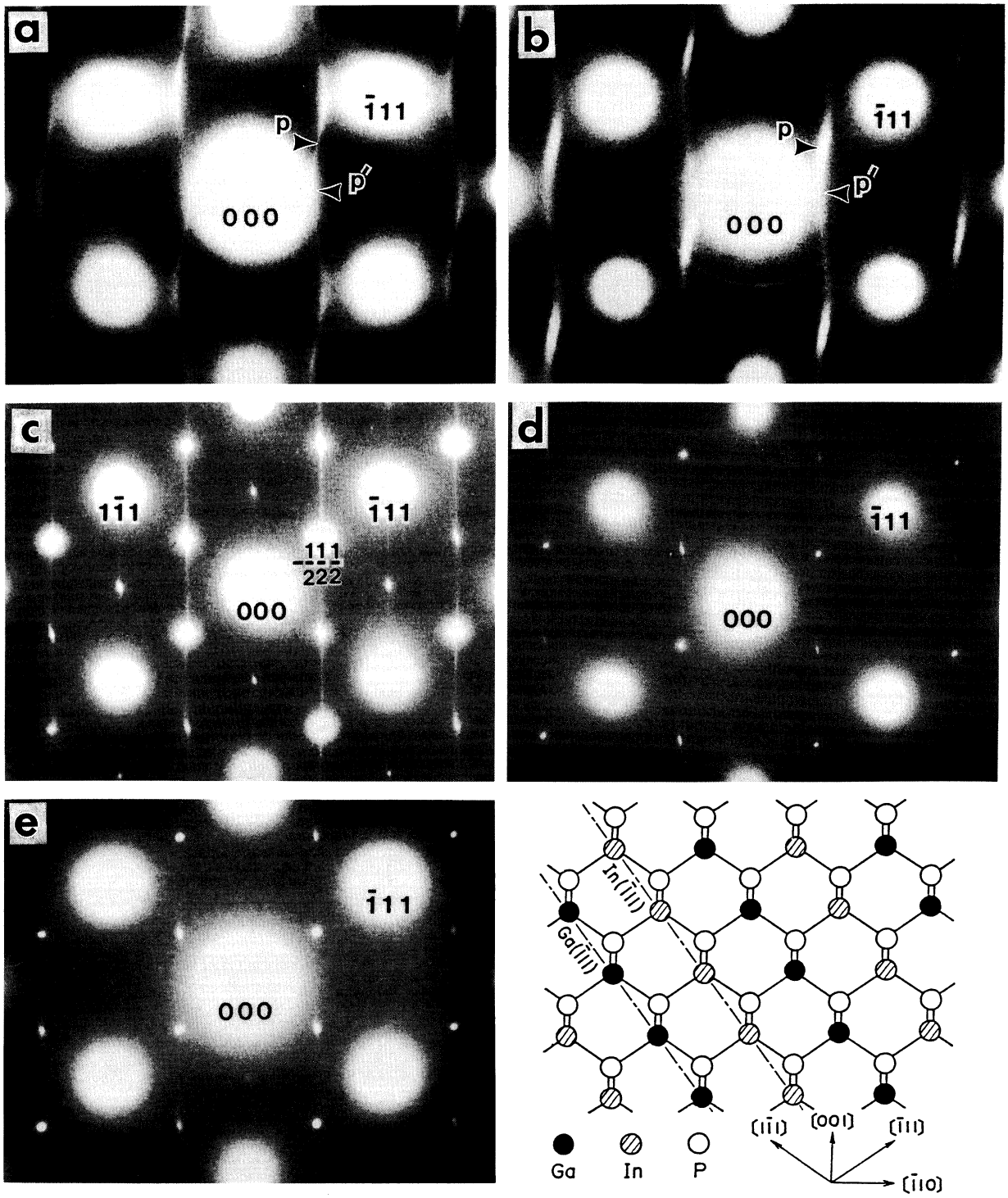

Fig. 7. [110] zone-axis TED patterns for $Ga_{0.5}In_{0.5}P$ grown under T_g (a) 550°C, (b) 600°C, (c) 700°C, (d) 750°C for ~400 V/III ratio, and (e) 700°C for 62 V/III ratio. These growth conditions correspond to those indicated by letters in Fig. 1. A structure model for the ($\bar{1}$11) SL projected to the [110] direction is shown (bottom right). P and P′ meanings are explained in the text (§3.2.1).

Under a V/III ratio ~400, superstructure spots at $-1/2, 1/2, 1/2$ in TED patterns showed maximum intensity for crystals grown at 650~700°C. As T_g becomes higher than 700°C, superstructure reflections remain spot-like in their shape, but the intensity becomes weaker as shown in Fig. 7(d). Samples grown at lower temperatures showed streaky and wavy diffuse scattering, as appears in Figs. 7(a) and 7(b). A 550°C case(a) shows extremely weak (virtually zero) intensity at $-1/2, 1/2, 1/2$ position (indicated by an arrow p) and the maxima of the diffuse scattering intensity rather shift towards the $-(1/2-\delta)$, $(1/2-\delta)$, 0, position indicated by an arrow p′, where d is a small positive number around 0.05. This shift can be recognized already for the 600°C case (Fig. 7(b)) in a less-pronounced manner; the diffuse scattering intensity maxima move slightly from the $-1/2, 1/2, 1/2$, position towards $-(1/2-\delta)$, $1/2-\delta$), 0. The δ value for the 600°C case is 0.03. The δ value becomes larger as T_g becomes lower from 700°C. At 700°C $0<\delta<0.004$. As T_g lowers from 700°C, the integral intensity for the extra reflections (super-structure spots or diffuse scatterings) other than the basic matrix spots ($\bar{1}$, 1, 1; 0, 0, 2; . . .) becomes weaker (Figs. 7(a) and 7(b)). Note the relative intensities between these extra reflections and the base matrix spots, *e.g.* the $\bar{1}$, 1, 1 spot. Thus, the superstructure shows a maximum intensity at T_g 650~700°C under V/III ratio ~400, where the long-range order of the ($\bar{1}11$) SL best develops. A sample with an anomalous E_g value, grown at T_g 650°C and V/III 230, also showed extremely strong superstructure spots.

Figure 7(e) shows a TED pattern for a T_g 700°C and V/III 62 case. The intensity at the $-1/2, 1/2, 1/2$ position is much weaker than that for the T_g 700°C and V/III ~400 case (Fig. 7(e)) and appears comparable to that for the T_g 750°C and V/III 400 case. The shape of the superstructure reflection is spot-like. The TED pattern for a crystal grown under T_g 700°C and V/III 130, which has an intermediate E_g value,[1] showed intermediate intensity $-1/2, 1/2, 1/2$ spots.

It is noticed that the exact positions of the previously reported $\mp 1/2, \pm 1/2, 0$, spots in the [001] zone axis[2] are $\mp(1/2-\delta')$, $\pm(1/2-\delta')$, 0, where δ' has a small positive value. Here, the δ' values for crystals grown under different conditions agree well with respective δ values mentioned above. Thus, the previously reported superspots can be interpreted as the intersections of the Ewald sphere in the [001] zone axis with the three-dimensional wavy streak rods.

In Figs. 8(a), 8(b), and 8(c), dark-field lattice (DFL) images recorded using an aperture including $-1/2, 1/2, 1/2$, $-1/2, 1/2, 3/2$ and $-1, 1, 1$ reflection points are shown for the same samples as in Figs. 7(a), 7(b), and 7(c), respectively. These photographs reveal the atomic arrangement change with the T_g change. For 700°C, the dominance of the ($\bar{1}11$) SL, which runs from the top left to the bottom right in Fig. 8(c), over that of the ($1\bar{1}1$) SL, is observed, which is consistent with the corresponding TED pattern (Fig. 7(c)). The periodicity is 6.5 Å, which is double that for $d_{\bar{1}11}$ It is noticed that there are some disordered regions (middle right) and ($\bar{1}11$) SL regions overlapped with ($1\bar{1}1$) SL (upper left). The latter overlapping

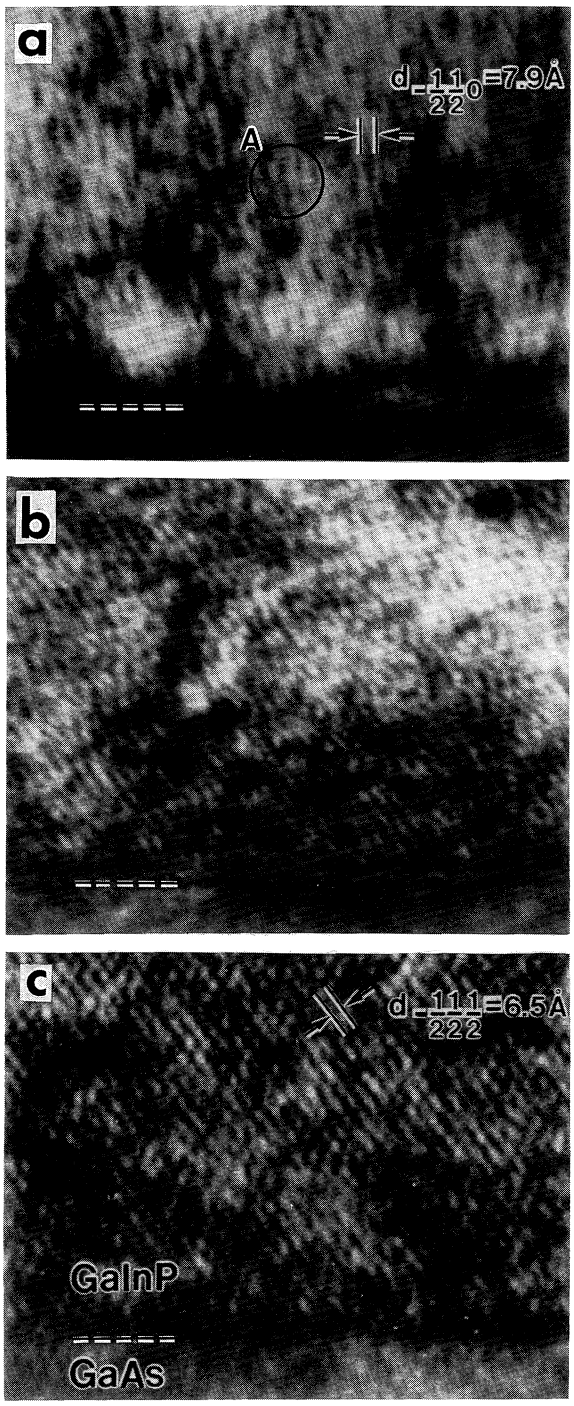

Fig. 8. Dark-field lattice images for $Ga_{0.5}In_{0.5}P$ grown under T_g (a) 550°C, (b) 600°C, (c) 700°C for ~400 V/III ratio. These samples are the same as those in Fig. 7(a), 7(b) and 7(c), respectively. A dotted line for each figure indicates an interface between the epilayer and the substrate. The meaning for portion A in (a) is explained in the text. $d_{-1/2,1/2,0}$ represents the lattice spacing for $(-1/2, 1/2, 0)$ planes.

structure is understood if we consider layered domains of ($\bar{1}11$) SL and ($1\bar{1}1$) SL, in the sample thickness direction, i.e. the [110] direction. In Fig. 9 a high-resolution TEM image for a relatively complete ($\bar{1}11$) SL portion is shown. A monolayer SL with 6.5 Å periodity in the [$\bar{1}11$] direction is observed. For 600°C, the DFL image Fig. 8(b) shows bunches of wavy lines and some disorders. Diffuse TED patterns very similar to the present 600°C case (Fig. 7(b)) have recently been reported in $Ga_{0.5}In_{0.5}P$

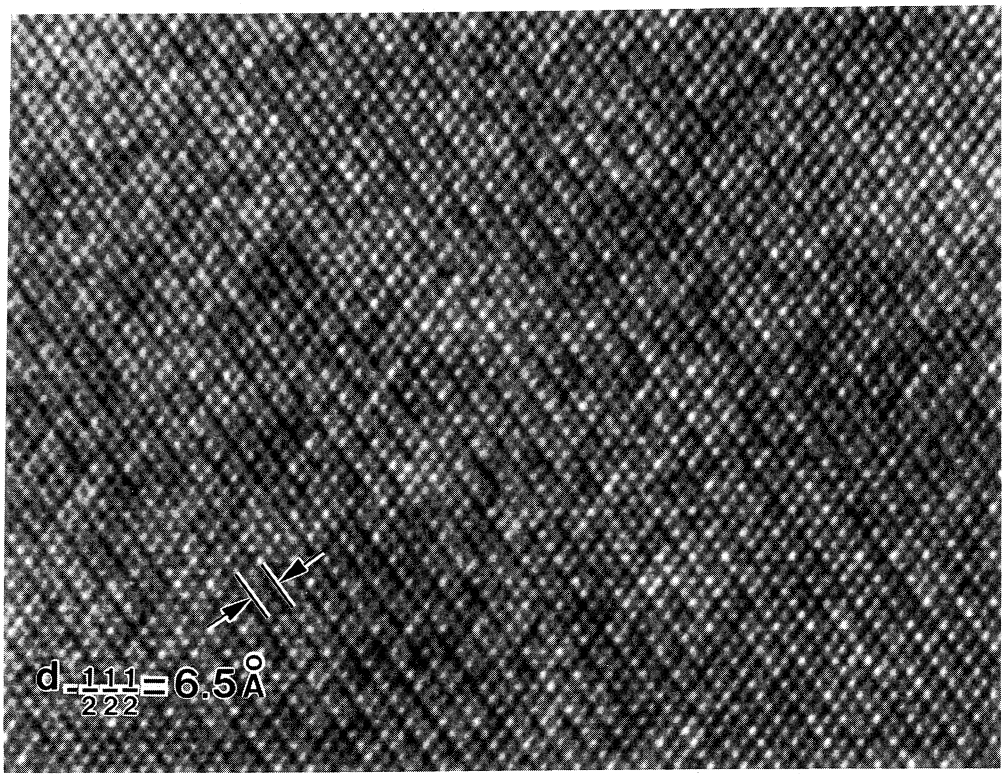

Fig. 9. High-resolution lattice image for the same sample as used in Fig. 8(c). T_g 700°C and V/III ratio 405.

grown by MOVPE.[10,11] For 550°C, the DFL image Fig. 8(a) also shows disorders and bunches of wavy lines, but whose directions are close to [001]. Deviations from a complete ($\bar{1}11$) SL can be explained by considering anti-phase boundaries (APBs), as is shown in the following.

Figures 10(a) and 10(b) show sublattice structure models for crystals grown at 700°C and lower temperatures, respectively.* This illustration is the projection to the (110) plane. A series of APBs (β_1, β_2, . . . between fractions of the ($\bar{1}11$) SL well simulates the observed DFL images for lower T_g values (Fig. 10(b)). A statistical variation in these APB intervals gives rise to the diffuse scatterings for lower T_g samples. As T_g lowers, the numbers of

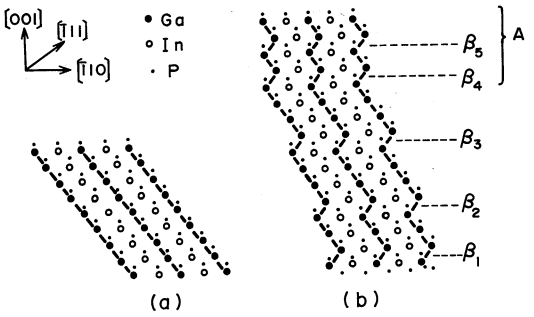

Fig. 10. Structure model projected to the (110) plane (a) for a well-developed ($\bar{1}11$) SL and (b) for a sublattice ordering seen in $Ga_{0.5}In_{0.5}P$ grown at lower temperatures. β_1, β_2, . . . indicate anti-phase boundaries between fractions of ($\bar{1}11$) superlattice (SL). The model simulates well, *e.g.*, the circled portion (A) in Fig. 8(a) DFL image.

*S. Iijima, A. Gomyo and T. Suzuki: Extended Abstracts of the 35th Spring Meeting of Jpn. Soc. Appl. Phys., Tokyo (1988)30p-Z3. (in Japanese).

APBs increase and, in turn, the average direction of the bunches of wavy lines becomes parallel to the [001] direction. The DFL image for the 550°C case (Fig. 8(a)) shows that most of the bunches of lines are nearly parallel to the [001] direction, and that their local periodicity is about 7.9 Å (*e.g.*, portion A encircled in the figure). This is consistent with the observation that the diffuse-scattering intensity maxima, for the 550°C case (Fig. 7(a)), are near the $\mp(1/2-\delta)$, $\pm(1/2-\delta)$, 0 positions.

The local periodicities observed in the DFL images (Fig. 8) vary from place to place statistically. They are approximately in the range between 6.5 and 7.9 Å. Here, 7.9 Å corresponds to the periodicity of, *e.g.* portion A in Fig. 10(b). Portion A can be interpreted to be a very small fraction of the bilayer SL reported previously.[2] Its coherence length is very small (less than a few tens of Å). The small positive δ value may be a result of small local atom displacements (expansion ratio $1+2\delta$), which might be caused by stress at the APBs. The δ value increases as T_g lowers. It is considered that the increased number of APBs, which arises from lowering T_g, results in the large lattice distortion (larger δ) around the APBs.

3.2.2 *$(Al_{0.4}Ga_{0.6})_{0.5}In_{0.5}P$ and $Al_{0.5}In_{0.5}P$*

Figures 11(a) and 11(b) show [110] zone-axis TED patterns for $(Al_{0.4}Ga_{0.6})_{0.5}In_{0.5}P$ and $Al_{0.5}In_{0.5}P$. The dominance of the ($\bar{1}11$) SL over the ($1\bar{1}1$) SL is observed in these figures, as is also the case for $Ga_{0.5}In_{0.5}P$. It was found that neither ($11\bar{1}$) nor ($\bar{1}\bar{1}\bar{1}$)SL was observed in the [$\bar{1}10$] zone-axis TED patterns. This observation is also the same as for $Ga_{0.5}In_{0.5}P$.

3.3 *Discussion*

As has been described in §3.1.1 and §3.2.1, we have ob-

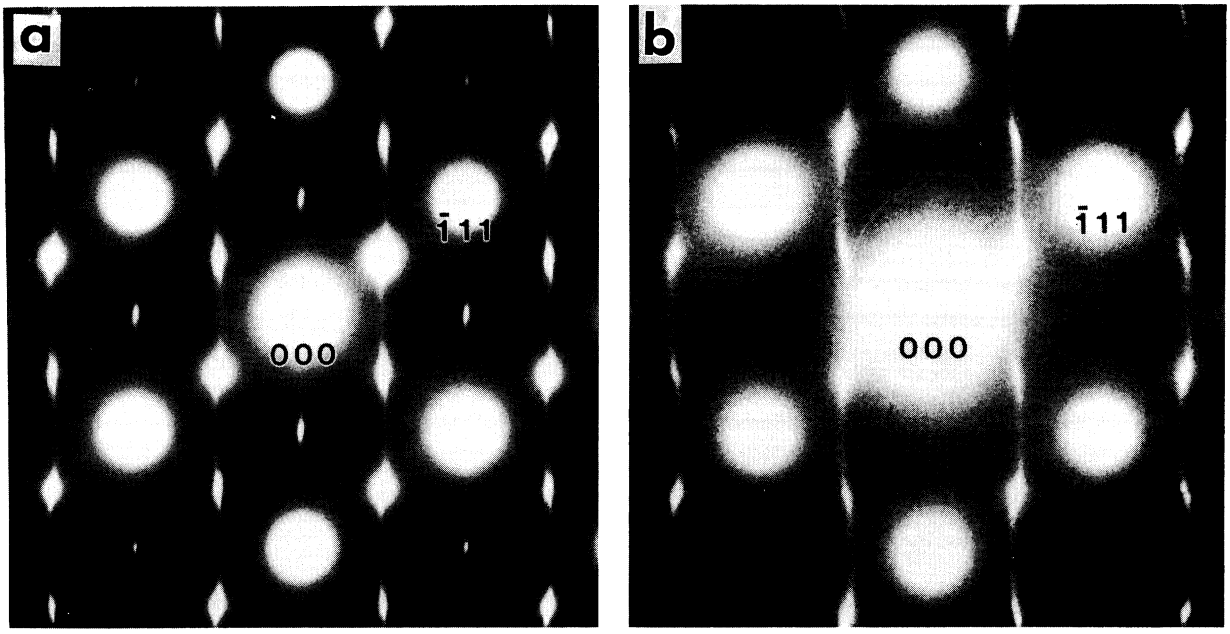

Fig. 11. [110] zone-axis TED patterns for (a) $(Al_{0.4}Ga_{0.6})_{0.5}In_{0.5}P$ and (b) $Al_{0.5}In_{0.5}P$. Growth conditions were (a) T_g 700°C and V/III 400, and (b) T_g 650°C and V/III 140, respectively.

served an excellent qualitative correlation between the superstructure intensity at the $-1/2$, $1/2$, $1/2$ position in the [110] zone axis and the degree of the E_g anomaly for $Ga_{0.5}In_{0.5}P$ prepared under a wide range of MOVPE growth conditions. This correlation has been observed for samples grown at T_g 700°C under the V/III ratios 62, 130 and ~400, as well as for a series of samples grown at T_g ranging from 550 to 750°C under V/III ratio ~400. In samples with the lowest E_g values 1.83~1.85 eV, the {111} SLs have best developed. These observations indicate that the {111} SLs are responsible for the anomalously low E_g value in $Ga_{0.5}In_{0.5}P$.

The previous report[2] suggested the correlation between the E_g anomaly and the $\mp 1/2$, $\pm 1/2$, 0 TED spot intensity in the [001] zone axis, based only on the observations for (A) T_g 650°C, V/III 222 and (B) T_g 700°C, V/III 58 samples. However, samples grown at lower T_g ((b) 600 and (a) 550°C) under V/III ~400 showed stronger intensity than that for condition (A), although E_gs for (a) and (b) show higher values, as shown in Fig. 1. The previously reported $\mp 1/2$, $\pm 1/2$, 0 spot intensity in the [001] zone axis monotonically increases as T_g lowers from 750 to 550°C under V/III ratio ~400, although the intensity even for 550°C is orders of magnitude weaker than that for the newly observed $\mp 1/2$, $\pm 1/2$, $1/2$ spot intensity for condition (c) shown in Fig. 1. Thus the previous suggestion for a correlation between the $\mp 1/2$, $\pm 1/2$, 0 spot intensity and the E_g anomaly should be corrected. The monotonic increase in the $\mp 1/2$, $\pm 1/2$, 0 spot intensity is understood to be a result of the intensity maximum shift from the $\mp 1/2$, $\pm 1/2$, $1/2$ position towards the $\mp(1/2-\delta)$, $\pm(1/2-\delta)$, 0 position. This shift is related to the increase in the APB density with the decrease of T_g.

The assertion that the anomalous E_g is correlated with the existence of the {111} SLs is also supported by other experimental materials: (1) it has been found that when the Zn impurity is diffused into the $Ga_{0.5}In_{0.5}P$ grown under the condition in which it takes an abnormal E_g value, the E_g value changed to a normal value.[2] This E_g change can be interpreted as an impurity-diffusion-enhanced randomization of the SL.[2] This interpretation is, in turn, supported by the fact that in a highly p-type impurity-(such as Zn) doped $Ga_{0.5}In_{0.5}P$ layer grown under the condition in which $Ga_{0.5}In_{0.5}P$ shows {111} SLs and takes an abnormal E_g value unless it is undoped, the crystal showed a normal E_g value[8] and, simultaneously, {111} SLs disappeared. (2) There are good correlations between the "valley depth b/a" and E_g (as shown in Fig. 5), and between peak Z (as shown in Fig. 4) and the E_g. In $Ga_{0.5}In_{0.5}P$ with the {111} SLs, phonons at the L point in the Brillouin zone will be folded to the Γ point. In Fig. 4, LO^*_L and LA^*_L indicate calculated zone-folded LO and LA phonons at the L point. LO_L and LA_L are calculated simply by averaging LO_L and LA_L phonon energies for GaP and InP with composition weighting, which have been obtained by neutron scattering experiments.[12,13] The calculated phonon energies are normalized to the experimentally observed LO_Γ phonon energy. The "valley" position and peak Z position are fairly near the calculated zone-folded LO and LA phonon energies at the L point. Thus, it is reasonable to assume a correlation between the anomalous E_g and the {111} SLs, through the correlations between the "valley depth b/a" and the E_g, and between the peak Z and the E_g. (3) A $Ga_{0.5}In_{0.5}P$ layer grown on a (111)B GaAs under a condition in which $Ga_{0.5}In_{0.5}P$ shows {111} SLs and takes an abnormal E_g value if it is grown on a (001) GaAs 2° off towards the [011] direction, did not show {111} SL at all and showed a normal E_g 1.9 eV.*

*A. Gomyo, T. Suzuki, S. Iijima, K. Kobayashi, S. Kawata, H. Fujii, and I. Hino: Extended Abstracts of the 35th Spring Meeting of Jpn. Soc. Appl. Phys., Tokyo (1988) 30p-Zl, Z2 (in Japanese). A paper reporting details has been submitted to Jpn. J. Appl. Phys.

It is noticed that, in Fig. 8(c), there are some disordered local regions (*e.g.*, in the middle right). Depending on the degree of disorder, the E_g for each disordered region may have corresponding different values. The disordered regions may thus be responsible for the broadness in the transmission spectrum for a sample with the E_g anomaly, as shown in Fig. 3.

These experimental facts all seem to support the assertion that the anomalous E_g is correlated to the {111} SLs, which has been made based on the observation of the correlation between the E_g and the {111} SLs for a wide range of $Ga_{0.5}In_{0.5}P$ growth conditions. The existence of the {111} SLs on the column III sublattice is considered to change the electronic energy band structure. The change will result in the experimentally observed E_g reduction. The present observation reminds us of a similar relation between E_g and SL for $Ga_{0.5}In_{0.5}As$ and artificially grown SL $(GaAs)_1(InAs)_1$ whose average composition is the same as that for $Ga_{0.5}In_{0.5}As$.[14] Both were grown on (001) InP by MOVPE. The E_g value for the sample with the artificially-formed (001) monolayer SL is reported to be ~ 30 meV lower than E_g for random $Ga_{0.5}In_{0.5}As$. Recently, Kurimoto and Hamada have performed first-principle self-consistent all-electron local-density band-structure calculations for the $(GaP)_1(InP)_1$ {111} SL and have actually shown a significant E_g reduction.[15] The cause of the E_g anomaly in $(Al_xGa_{1-x})_{0.5}In_{0.5}P$ is considered to be the same as that for the $Ga_{0.5}In_{0.5}P$ case.

GaAs substrate-surface orientation effects on {111} SLs formation have been studied. Based on these studies, a {111} SL formation mechanism in $(Al_xGa_{1-x})_{0.5}In_{0.5}P$ ($x=0$, $0<x<1$, and $x=1$) has been described in a separate paper.[16] The growth condition dependence of the sublattice ordering described in the present work is also discussed.

§4. Summary and Conclusion

Detailed data for the photoluminescence (PL) peak energy anomaly for $Ga_{0.5}In_{0.5}P$ was presented as a function of a wide-range of MOVPE growth conditions: the growth temperature (T_g) ranging from 550°C to 750°C and the V/III ratio ranging from 60 to ~ 400. Alloy compositions determined by lattice-mismatch measurements using X-ray diffractions and Vegard's law were compared to those determined by X-ray microanalysis. The former method, which uses lattice-mismatch measurements, was found to represent well the alloy composition even for the crystals with anomalous PL peak energies. The PL peak anomaly was found to occur even in epilayers with lattice mismatches of at least up to 7×10^{-3}.

Optical transmission spectra measurements were carried out for crystals with normal and anomalous PL peak energies. The spectra showed band-gap absorption edges, displaced by approximately the same energy as the PL peak energy difference. It is thus reconfirmed that the PL peak energy can be considered to represent the band-gap energy (E_g).

Structure analysis by TEM was performed. TED patterns and DFL images for samples grown under various growth conditions were analyzed. A relation between the superstructures observed in the [001] and [110] zone axes was discussed. It was confirmed that the {111} SL on the column III sublattice is responsible for the E_g anomaly.

The previously reported relation between E_g and "valley depth" in Raman scattering spectra was observed for samples with a wide range of growth conditions. A new peak was reported at 207 cm^{-1} and correlated with the E_g anomaly. The "valley depth" and 207 cm^{-1} was interpreted as a result of Brillouin-zone folding due to the {111} SL observed in the anomalous E_g samples.

A similar E_g anomaly was reported for AlGaInP. Structure analyses for AlGaInP and AlInP were performed and the existence of the {111} SLs was reported.

Acknowledgements

The authors are indebted to H. Fujii, H. Hotta, Y. Ueno, and T. Kawamura for growing part of the MOVPE crystals used in the present study and helpful discussions, and to T. Sato and J. Nakajima for XMA measurements. They would like to thank M. Sakaguchi for continuous encouragement. They also would like to thank Akashi Beam Technology Ltd. for the use of an electron microscope.

References

1) A. Gomyo, K. Kobayashi, S. Kawata, I. Hino, T. Suzuki and T. Yuasa: J. Cryst. Growth **77** (1986) 367.
2) A. Gomyo, T. Suzuki, K. Kobayashi, S. Kawata, I. Hino and T. Yuasa: Appl. Phys. Lett. **50** (1987) 673.
3) Y. Oba, M. Ishikawa, H. Sugawara, M. Yamamoto and T. Nakanishi: J. Cryst. Growth **77** (1986) 374.
4) H. Asai and K. Oe: J. Appl. Phys., **53** (1982) 6849.
5) C. P. Kuo, S. K. Vong, R. M. Cohen, and G. B. Stringfellow: J. Appl. Phys., **57** (1985) 5428.
6) R. J. Nelson and N. Holonyak, Jr.: J. Phys. Chem. Solids **37** (1976) 629.
7) T. Suzuki: Oyo Buturi **56** (1987) 990 (in Japanese).
8) T. Suzuki, A. Gomyo, K. Kobayashi, S. Kawata, I. Hino and T. Yuasa: IECE Tech. Rep. OQE87-45 (1987) 109 (in Japanese).
9) A. Gomyo, T. Suzuki and S. Iijima: Phys. Rev. Lett. **60** (1988) 2645.
10) O. Ueda, M. Takikawa, J. Komeno and I. Umebu: Jpn. J. Appl. Phys. **26** (1987) L1824.
11) P. Bellon, J. P. Chevalier, G. P. Martin, E. Dupont-Nivet, C. Thievaut and J. P. Andre: Appl. Phys. Lett. **52** (1988) 567.
12) P. H. Borcherds, K. Kunc, G. F. Alfrey, R. L. Hall: J. Phys. C: Solid State Phys. **12** (1979) 4699.
13) P. H. Borcherds, G. F. Alfrey, D. H. Saunderson and A. D. B. Woods: J. Phys. C: Solid State Phys. **8** (1975) 2022.
14) T. Fukui and K. Oe: J. Appl. Phys. **53** (1984) L527.
15) T. Kurimoto, and N. Hamada: to be published in Phys. Rev. B (1989).
16) T. Suzuki, A. Gomyo and S. Iijima: to be published in J. Cryst. Growth.